The object of this study is a powder tape for arc surfacing of composite and complex-alloyed alloys. Essentially, the peculiarities of their design determine the uneven heating and melting of the shell and core during the arc surfacing process. This causes chemical heterogeneity of the surfacing metal, which leads to a spread of its mechanical properties. Taking into account the thermal balance of heating the powder tape protrusion by the welding current during surfacing, a mathematical model has been built. It allows for a reliable and operational assessment of thermal effects depending on the welding current density, geometric dimensions, the filler metal filling ratio of the tape and the thermophysical characteristics of the metal shell and ingredients. Its quantitative accuracy makes it possible to predict general patterns of temperature differences, changes in the aggregate state, heat and mass transfer, and phase transitions. It also allows for the calculation of the direction and limits of physicochemical reactions and the identification of ways to control the power parameters of the powder tape manufacturing process and the characteristics of the surfacing mode.

Comparison of the calculated values of the average heating temperature with experimental data indicates the adequacy of the mathematical model and its feasibility for practical calculations. The data reported in the paper correctly reflect the nature of the heating of the powder tape, taking into account the composition of the core, the thickness of the shell, the size of the tape, the degree of compression of the metal shell and the powder core in the two-roll mill stand. Analytical description of the heating patterns makes it possible to solve under industrial conditions the technological tasks of improving the quality of the deposited metal, increasing the productivity of the process, as well as resource and energy saving when surfacing composite and alloyed wear-resistant alloys

Keywords: powder tape, thermal state, core, surfacing, composite alloy, alloyed alloy

UDC 621.791.75
DOI: 10.15587/1729-4061.2025.327904

FEATURES OF HEATING AND MELTING OF POWDER TAPE FOR SURFACING OF COMPOSITE AND COMPLEX-ALLOYED ALLOYS

Valeriy Kassov
Doctor of Technical Sciences, Professor
Department of Hoisting and Transport and Metallurgical Machines*
Olena Berezshna
Doctor of Technical Sciences, Professor
Department of Industrial Process Automation*
Svitlana Yermakova
Corresponding author
PhD
Department of Hoisting and Transport and Metallurgical Machines*
E-mail: svetlanayermakovaddmaptm@gmail.com
Dmytro Turchanin
PhD Student
Department of Hoisting and Transport and Metallurgical Machines*
Svetlana Malyhina
PhD, Associate Professor
Department of Computer Information Technologies*
*Donbass State Engineering Academy
Akademichna str., 72, Kramatorsk, Ukraine, 84313

Received 13.12.2024
Received in revised form 06.02.2025
Accepted 25.03.2025
Published 21.04.2025

How to Cite: *Kassov, V., Berezshna, O., Yermakova, S., Turchanin, D., Malyhina, S. (2025). Features of heating and melting of powder tape for surfacing of composite and complex-alloyed alloys. Eastern-European Journal of Enterprise Technologies, 2 (1 (134)), 60–67. https://doi.org/10.15587/1729-4061.2025.327904*

1. Introduction

The main directions of economic development under current conditions involve improving the quality of manufactured products and designing effective technological processes. The implementation of the planned activities, as the experience of developed countries shows, is impossible without the use and further development of surfacing. In the context of saving energy resources, scarce and expensive materials, the role of surfacing as a means of increasing the durability of quickly wearing machine parts and their multiple renewal is a priority [1]. Surfacing with powder tapes is one of the effective resource-saving methods for regenerating structural dimensions and strengthening by applying special alloys that have high wear resistance and ensure long-term preservation of the optimal geometry of the working body [2, 3]. Meeting the regulations for operational reliability of the surfacing metal, the ability to withstand various types of wear, compliance with the principles of interchangeability and economic feasibility are largely determined by the quality of the powder electrode and the metal surfacing with it [4]. Therefore, studies aimed at heating and surfacing of the powder tape are relevant.

2. Literature review and problem statement

In [5] it is shown that powder tapes are manufactured by rolling a metal shell with a continuous powder alloying charge and its subsequent compaction. In [6] it is shown that the design feature determines the multifactorial nature and

interrelation of the phenomena occurring during the heating of its individual components. This is especially true for the multicomponent powder composition of the core [7]. However, the lack of consideration of the influence of the thermophysical characteristics of the core and shell on the formation of heat flows does not make it possible to adequately assess the thermal environment in the heating zone.

In [8], a number of chemical compounds included in the charge become unstable at temperatures and do not lead to melting of the core and shell. Therefore, it is important to take into account not only the melting process of the powder electrode, considered in [6], but also the process of its heating. In [9] it is shown that the use of exothermic mixtures in the charge activates heating and melting due to the release of additional heat during the exothermic reaction in the core. However, guaranteeing the required composition of the deposited metal is limited due to the recovery of the oxidant components and its subsequent transition to slag [10]. In [11], modern trends in development and prospects for the use of powder electrodes are shown, but the ways of controlling the uniformity of heating and melting of the shell and core are not indicated. The processes in the weld pool are largely secondary to the processes in the powder electrode, which is not taken into account in [10, 11] when devising the deposition technology. This does not make it possible to apply the recommendations compiled when surfacing composite alloys, when the charge contains refractory metals. Their transition to the deposited layer in the initial state is not ensured. Predicting the quality of the layer only from the deposition mode [12] does not take into account the uneven heating and melting of the powder electrode. This is the cause of the chemical heterogeneity of the seam during the surfacing of alloyed wear-resistant alloys.

In this regard, it is advisable to conduct a study aimed at determining the thermal state of the powder tape during the surfacing of alloyed wear-resistant alloys.

3. The aim and objectives of the study

The purpose of our study is to determine the features of the thermal state of the powder tape during the surfacing of composite and complex alloyed alloys. This will make it possible to solve technological problems related to the quality of the deposited metal, increasing the productivity of the process, as well as resource and energy saving under industrial conditions.

To achieve the goal, the following tasks were set:

– to build a mathematical model of the thermal state of the metal shell of the powder tape taking into account geometric parameters, thermophysical properties, and surfacing modes;

– to compare the calculated values of the heating temperature of the shell of the powder tape with experimental data.

4. The study materials and methods

The object of our study is a powder tape for arc surfacing of composite and complex-alloyed alloys.

The principal hypothesis assumes that the adequacy of the mathematical model of the thermal state during surfacing and its reasonable accuracy for practical calculations could be ensured by taking into account the geometric parameters, thermophysical properties of the powder tape, and surfacing modes. To calculate the thermal state of the protrusion, a rectangular cross-section of the powder tape was adopted. When modeling the heating of the powder tape shell, the following initial data were determined, according to [13, 14]:

1. The electrical resistance of the core charge is much greater than the resistance of the powder tape shell, so the welding current passes mostly through the shell of the tape, and the current density in the powder tape can be calculated from the cross-section of the shell.

2. During the passage of the welding current through the powder tape, all the heat is released in its shell. The heat released is used to heat the shell, the core and is partially lost through the side surface of the powder tape by heat transfer to the environment. For the calculation, due to the small thickness of the bonding layer, a linear decrease in temperature along the thickness of the layer was adopted as a simplification.

Lock joints are taken into account when calculating the cross-sectional area of the powder tape shell. The studies were conducted for powder tapes of two classes: for surfacing alloyed alloys of the sormite type and composite type of rhelite-cupric iron. For surfacing of the sormite alloy, a complex alloy was introduced into the core of the powder tape. Geometric dimensions of the powder tape: width $b=20.0$ mm, thickness $h=4.0$ mm, thickness of the tape shell $\delta=0.4$ mm. The fill factor was 0.55, the tape shell was made of 08 kp steel. The composite alloy surfacing was provided by a powder tape containing a mechanical mixture of components in the core: rhelite, nickel, manganese, aluminum-magnesium powder. The fill factor was 0.75, the tape shell was made of copper. Geometric dimensions of the powder tape: $b=20.0$ mm, $h=4.0$ mm, $\delta=0.4$ mm. When studying the heating temperature of the powder tape shell on the ADF-1004 welding machine, thermocouples made of chromel-alumel wire with a diameter of 0.15 mm were installed in the middle of the powder tape shell. Measurements of the welding current and heating temperature were recorded with an oscilloscope K12-22.

5. Results of investigating the thermal state of the powder tape during surfacing

5. 1. Modeling the thermal state of the metal shell of the powder tape

The width b and the thickness h of the core are interconnected with the width and thickness of the powder tape through the thickness of the shell δ and the thickness of the connecting layer δ_l (if any) between the charge and the shell (Fig. 1).

The thermal balance of heating a section of powder tape by welding current, taking into account the assumptions adopted, is expressed by the following equation:

$$dQ = dQ_{sh} + dQ_c + dQ_l + dQ_s, \quad (1)$$

where dQ is the Joule heat released in the tape shell at this section of the protrusion; dQ_{sh} is the increase in the heat capacity of the tape shell; dQ_c is the increase in the heat capacity of the core of the powder tape; dQ_l is the increase in the heat capacity of the connecting layer between the shell and the charge; dQ_s is the heat transfer from the side surface of this section of the powder tape protrusion to the environment.

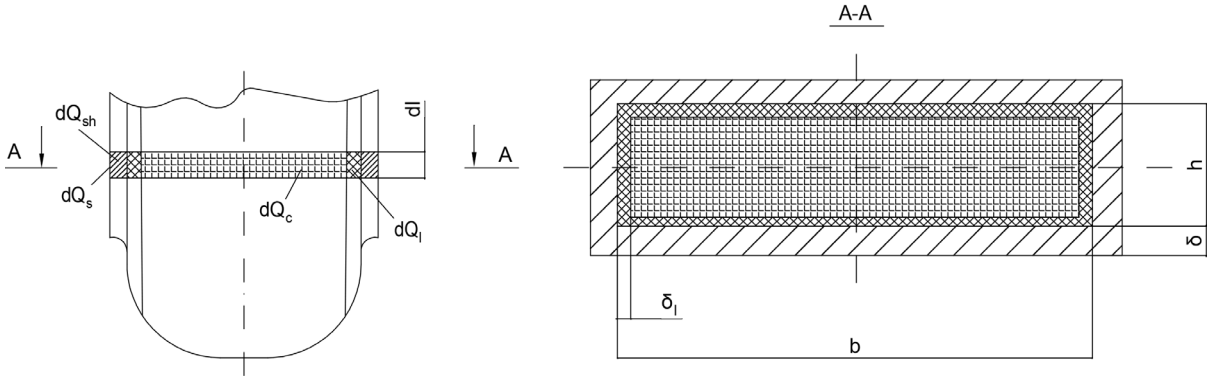

Fig. 1. Estimation diagram of powder tape

During the passage of current in the element *dl* of the protrusion shell (Fig. 1), heat will be released during the time *dt*:

$$dQ = \frac{\rho dl}{S_o} I^2 dt, \tag{2}$$

where ρ is the resistivity of the shell material, Ohm m; S_o is the cross-sectional area of the powder tape shell, m^2; I is the surfacing current, A.

The heat accumulation in the element *dl* of the protrusion shell during an increase in temperature by dT per unit time for a time *dt* will be:

$$dQ_{sh} = c_o \gamma_o \frac{dT}{dt} S_o dl dt, \tag{3}$$

where c_o – specific heat capacity (J/kg·degree); γ_o – density (kg/m^3) of the powder tape shell.

The heat accumulation in the element *dl* of the protrusion core when the charge temperature increases by dT_c per unit time for time *dt* will be:

$$dQ_c = c_c \gamma_c \frac{dT_c}{dt} S_c dl dt, \tag{4}$$

where c_c – specific heat capacity (J/kg·degree); γ_c – density (kg/m^3) of the core of the powder tape; S_c – cross-sectional area of the core of the powder tape, m^2.

The heat accumulation in the element *dl* of the bonding layer in the event of an increase in temperature by $d\overline{T_n}$ per unit time for time *dt* will be:

$$dQ_l = c_l \gamma_l \frac{d\overline{T_l}}{dt} S_l dl dt, \tag{5}$$

where c_l – specific heat capacity (J/kg·degree); γ_l – density (kg/m^3) of the binding layer material.

The heat given off from the lateral surface of the powder tape protrusion section *dl* during the time *dt* will be:

$$dQ_s = \alpha\left(T - T_o\right) P dl dt, \tag{6}$$

where α is the heat transfer coefficient with the environment, W/(m^2·degree); T is the heating temperature of the powder tape, degree; T_0 is the ambient temperature, degree; P is the perimeter of the powder tape, m.

Substituting the values of dQ, dQ_{sh}, dQ_c, dQ_l and dQ_s into equation (1), we obtain:

$$c_o \gamma_o \frac{dT}{dt} S_o = \frac{I^2}{S_0} \rho - c_c \gamma_c \frac{dT_c}{dt} S_c - \\ - c_l \gamma_l \frac{d\overline{T_l}}{dt} S_l - \alpha\left(T - T_o\right) P. \tag{7}$$

Since the connecting layer has a small thickness ($\delta_l \leq 0.1$–0.2 mm), which is an order of magnitude lower than the thickness of the core of the powder tape, it can be assumed that the temperature along the thickness of the connecting layer decreases linearly. And at the point of contact with the charge, the core of the layer has a temperature equal to:

$$T_l = wT, \tag{8}$$

where the coefficient w is in the range $0 < w \leq 1$, and $w=1$ if there is no connecting layer. Then the average temperature of the connecting layer $\overline{T_l}$ will be equal to:

$$\overline{T_l} = 0.5\left(T + T_l\right).$$

Substituting the value of T_l from formula (8), we obtain:

$$\overline{T_l} = 0.5\left(1 + w\right) T. \tag{9}$$

Then:

$$\frac{d\overline{T_l}}{dt} = 0.5\left(1 + w\right) \frac{dT}{dt}.$$

Assuming that the average heating rate of the powder tape core is proportional to the heating rate of the shell:

$$\frac{dT_A}{dt} = wm \frac{dT}{dt},$$

equation (7) can be simplified. As a result, the following was obtained:

$$\left(c_o \gamma_o + wmc_c \gamma_c \frac{S_c}{S_o} + 0.5\left(1 + w\right) c_l \gamma_l \frac{S_l}{S_o} \right) \frac{dT}{dt} = \\ = \frac{I^2}{S_o^2} \rho - \alpha\left(T - T_o\right) \frac{P}{S_o}.$$

By denoting:

$$j = \frac{I}{S_o},$$

$$A = c_o \gamma_o + wmc_c \gamma_c \frac{S_c}{S_o} + 0.5\left(1 + w\right) c_l \gamma_l \frac{S_l}{S_o}, \tag{10}$$

we obtained:

$$A\frac{dT}{dt}=\rho j^2-\alpha\left(T-T_o\right)\frac{P}{S_o}. \quad (11)$$

The resistivity of the powder tape shell is a function of temperature and is described by the following formula:

$$\rho=\rho_o\cdot\left(1+\beta T\right), \quad (12)$$

where ρ_0 is the resistivity at the initial temperature, Ohm m; β is the temperature coefficient of the shell resistance, degree^{-1}.

Substituting (12) into equation (11), we obtain:

$$\frac{dT}{dt}=\frac{\rho_o\beta j^2-\alpha P/S_o}{A}T+\frac{\rho_o j^2+\alpha PT_o/S_o}{A}. \quad (13)$$

Let's enter the designation:

$$k=\frac{\rho_o\beta j^2-\alpha P/S_o}{A},$$

$$B=\frac{\rho_o j^2+\alpha PT_o/S_o}{A}, \quad (14)$$

$$C=\frac{B}{k}=\frac{\rho_o j^2+\alpha PT_o/S_o}{\rho_o\beta j^2-\alpha P/S_o}.$$

Then equation (13) can be written as:

$$\frac{dT}{dt}=kT+B. \quad (15)$$

Differential equation (15) should be solved by the method of dividing variables. Then:

$$\frac{dT}{kT+B}=dt.$$

Hence:

$$\ln\left(kT+B\right)=kt+\ln\left(kT_o+B\right),$$

$$\ln\frac{kT+B}{kT_o+B}=kt,$$

$$\frac{kT+B}{kT_o+B}=e^{kt},$$

$$T=\frac{1}{k}\left(\left(kT_o+B\right)e^{kt}-B\right),$$

$$T=\frac{B}{k}e^{kt}+T_oe^{kt}-\frac{B}{k}.$$

Using the notation (14), finally:

$$T=T_o+\left(C+T_o\right)\left(e^{kt}-1\right). \quad (16)$$

To determine the temperature of the protrusion cross-section located at a distance L (m) from the power supply, it is necessary to substitute the heating time value into formula (16):

$$t=L/\nu,$$

where ν is the melting (feeding) speed of the powder tape, m/s.

Then the last equation is written as:

$$T=T_o+\left(C+T_o\right)\left(e^{kL/\nu}-1\right). \quad (17)$$

When solving the heat balance equation, the values of the specific heat capacities of the shell c_o, the charge c_c, and the connecting layer c_l are taken as averaged over the calculated temperature range.

When denoting the ratio of the core mass to the shell mass by K_c:

$$K_c=\frac{\gamma_c S_c}{\gamma_o S_o},$$

and the ratio of the mass of the connecting layer to the mass of the tape shell through K_l:

$$K_l=\frac{\gamma_l S_l}{\gamma_o S_o}.$$

Then we can convert formula (10) for calculating the coefficient A to the following form:

$$A=\gamma_o\left(c_o+wmK_cc_c+0.5\left(1+w\right)K_lc_l\right). \quad (18)$$

And the coefficient k in formula (17) can be determined from the following expression:

$$k=\frac{\rho_o\beta j^2-\alpha P/S_o}{\gamma_o\left(c_o+wmK_cc_c+0.5\left(1+w\right)K_lc_l\right)}, \quad (19)$$

where $P=2\left(b+h+4\delta\right)$, m;

$$S_o=2\delta\left(b+h+2\delta+\frac{hl}{2}\right),\ \text{m}^2\ \text{(Fig. 1)}.$$

The presented set of analytical descriptions made up a complete algorithm for mathematical modeling of the process of heating the powder tape. In order to confirm the adequacy of the constructed mathematical model, computational and experimental studies on the thermal state of the powder tape along the length of the offset for various shell materials were carried out.

5. 2. Comparison of theoretical and experimental studies on the thermal state of the powder tape

During the calculation, the following values were accepted: $b=20$ mm, $h=4$ mm, $\delta=0.4$ mm, $n=6$. In this case, the perimeter of the shell is 51.2 mm, and the cross-sectional area of the shell is 20.8 mm^2. The coefficient of uneven heating of the core m was taken equal to 0.8, and the specific heat capacity of the charge c_c according to [15] was taken equal to $c_c=0.6c_o$. In the case of a steel shell, the calculation considered: $c_o=460$ J/(kg·degree), $\gamma_o=7.8\cdot10^3$ kg/m^3, $\rho_0=0.14\cdot10^{-6}$ Ω·m, $\beta=6\cdot10^{-3}$ degree^{-1}; for copper shell: $c_o=396$ J/(kg·degree), $\gamma_o=8.9\cdot10^3$ kg/m^3, $\rho_0=0.058\cdot10^{-6}$ Ohm·m, $\beta=4\cdot10^{-3}$ degree^{-1}. The heat exchange coefficient with the environment α according to [16] was taken as 17 W/(m^2·degree).

By studying formula (16) and expressions (14) and (19) for calculating the model parameters, the dependences of the heating of the powder tape shell on the welding current density and the powder tape filling coefficient were determined (Fig. 2–4).

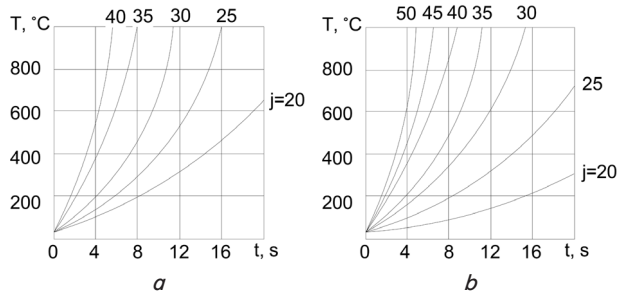

Fig. 2. Calculated heating temperatures of the powder tape shell depending on the density and time of current flow: *a* – powder tape at K_f=0.3; *b* – powder tape at K_f=0.6

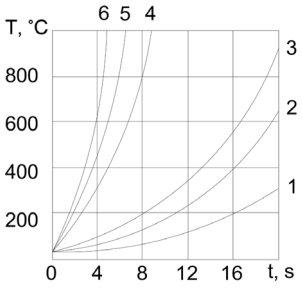

Fig. 3. Calculated heating curves of the powder tape shell depending on the current flow time and the fill factor K_f: 1, 2, 3 – current density 20 A/mm^2; 4, 5, 6 – current density 40 A/mm^2; 1, 4 – K_f=0.5; 2, 5 – K_f=0.3; 3, 6 – K_f=0

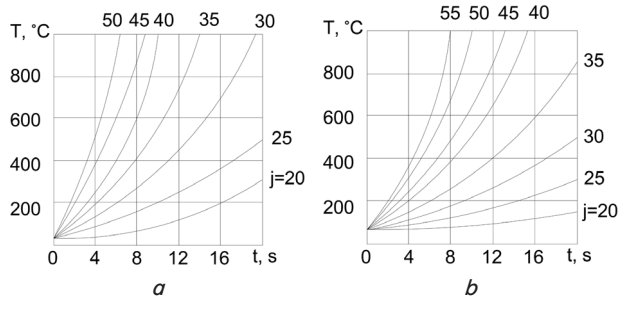

Fig. 4. Calculated heating curves of the copper shell of the powder tape depending on the density and time of current flow: *a* – powder tape at K_f=0.3; *b* – powder tape at K_f=0.6

Table 1 gives calculation of the heating temperature of the powder tape shell (K_f=0.6) with and without taking into account the heat dissipation by the side surface of the tape protrusion. Table 2 gives the calculated values of the relative reduction (in %) of the heating temperature of the powder tape shell when the heat dissipation of the side surface is taken into account.

Table 1

Powder tape shell heating temperature

α, W/(m^2·degree)	*j*, A/mm^2	Shell heating temperature (°C), during heating time (s)			
		4	6	8	10
17	25	93	139	193	255
	30	134	213	313	439
	35	190	324	510	763
	40	268.5	496	840	1,360
0	25	94	142	198	264
	30	136	218	322	456
	35	193	332	526	794
	40	273	508	868	1,420

Table 2

Relative reduction in the heating temperature of the shell when taking into account heat transfer by the lateral surface of the powder tape

j, A/mm^2	Percentage of temperature decrease during shell heating time, s			
	4	6	8	10
25	1.1	2.2	2.5	3.4
30	1.5	2.3	2.8	3.7
35	1.6	2.4	3.0	3.9
40	1.6	2.4	3.2	4.2

Our results make it possible to calculate the temperature at any point of the powder tape when performing the surfacing of composite and complex-alloyed alloys.

To experimentally confirm the mathematical model of the thermal state of the powder tape protrusion, studies were conducted to determine the heating temperature of the powder tape shell depending on the duration of melting process (Fig. 5).

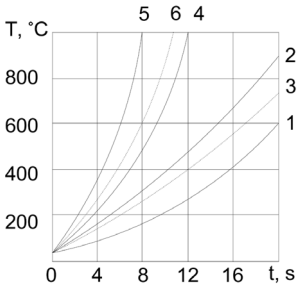

Fig. 5. Heating temperature of the powder tape shell depending on the current flow time (I=700 A): 1 – heating of the middle part of the copper shell; 2 – heating of the locking connection of the copper shell; 3 – calculated heating curve of the copper shell; 4 – heating of the middle part of the steel shell; 5 – heating of the locking connection of the steel shell; 6 – calculated heating curve of the steel shell

Comparison of the calculated values of the average heating temperature of the powder tape shell with experimental data shows their good agreement. This makes it possible to conclude that the calculation scheme is correct and that formulae (14), (16), (19) are reasonably accurate for practical purposes.

A study was also conducted to determine the heating temperature of the shell metal at the protrusion of the powder tape during the melting process. The parameters of the surfacing mode with powder tapes manufactured with different compression forces are given in Table 3.

Table 3

Surfacing modes

Material	Experiment number	Powder tape rolling force, kN	Surfacing modes	
			Welding current I, A	Voltage U, V
Powdered tape for surfacing of sormite alloy	1	5	700	31
	2	10	700	31
	3	15	710	31
	4	20	730	30
	5	25	750	29
Powdered tape for surfacing of relite-cupric iron alloy	6	5	520	35
	7	10	550	34
	8	15	580	33
	9	20	600	32
	10	25	620	32

The surfacing rate of the high-alloyed alloy sormite was 30 m/h, and of the composite alloy relite-cupric iron – 16 m/h. The length of the measured piece of powder tape was 300 mm, the electrode protrusion – 60 mm. The melting rate of the powder tape decreases with increasing degree of compression, and the heating time of the protrusion of the powder tape with a steel shell is 5–6 s, and with a copper shell – 8–10 s (Table 4).

Table 4

Melting rate and heating time of powder tape protrusion

Experiment number	Time of surfacing s, s	Surfacing speed, mm/s	Protrusion heating time, s
1	24.2	12.4	4.8
2	28.3	10.6	5.7
3	29.0	10.3	5.8
4	27.8	10.8	5.6
5	28.0	10.7	5.6
6	37.4	8.0	7.5
7	41.6	7.2	8.3
8	45.2	6.6	9.0
9	47.0	6.4	9.4
10	52.7	5.7	10.5

The results of experimental studies of the thermal state of the powder tape protrusion depending on the shell material are shown in Fig. 6.

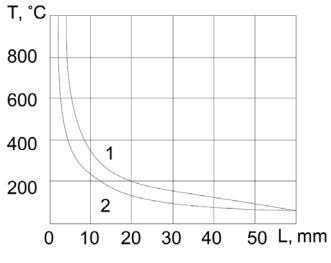

Fig. 6. Temperature distribution at the protrusion of the powder tape during surfacing: 1 — heating temperature of the steel shell (experiment 4); 2 — heating temperature of the copper shell (experiment 9)

The results of measuring the heating temperature of the powder tape protrusion by welding current showed that the heating temperature of the powder tape protrusion with a length of 40–80 mm during its melting is in the range of 400–600 °C for a steel shell, and 300–400 °C for a copper shell.

6. Discussion of results based on the theoretical and experimental research into the thermal state of the powder tape during surfacing

A feature of the reported mathematical model (16) and expressions (14), (17) to (19) is the presence of a connecting layer δ_l between the charge and the shell (Fig. 1), namely, taking into account the accumulation of heat dQ_l in the element dl of the connecting layer (5). In this case, the specific heat capacity c_l and the density of the material of the connecting layer γ_l are taken into account. That made it possible to determine the average temperature of the layer T_l (9). Thus, our mathematical model (16) and expressions (14), (17) to (19) make it possible to determine the dependence of the heating temperature of the shell protrusion not only on the welding current density, the size of the fill factor, and the thermophysical properties of the shell material and the core but also taking into account the thermophysical properties of the connecting layer.

Analysis of the results from computational studies (Fig. 2, 3) according to the proposed mathematical model reveals that with equal values of welding current and heating time, i.e., the same amounts of heat released in the tape shell, the heating temperature of the powder tape protrusion without charge (K_f=0) is higher than with charge (K_f=0.3; 0.6). Therefore, part of the heat released in the shell is spent on heating the core of the powder tape, which reduces the heating temperature of the shell at the protrusion of the powder tape.

In addition, our calculations carried out according to the proposed analytical expressions show that with an increase in the temperature and duration of heating of the powder tape, heat losses due to heat dissipation of the side surface increase.

The results of theoretical and computational studies were confirmed by experimental data. This indicates the reliability of the selected calculation scheme and the possibility of applying our analytical dependences for the purpose of practical assessment of the thermal state of the powder tape at the stage of designing the surfacing technology.

From the analysis of experimental results (Fig. 5), it was found that the heating temperature along the perimeter of the shell is not uniform. In the lock joints, higher heating is characteristic than in the central part of the powder tape. Moreover, the temperature difference increases uniformly with increasing temperature. This can be explained by the difference in the current flow along the perimeter of the powder tape shell. More than 30 % of the welding current flows through the locks. With increasing current density, the temperature difference along the perimeter of the shell increases. At a current density of up to 30 A/mm^2, the temperature difference is up to 100 °C, and in the case of increasing current density to 40 A/mm^2, the temperature difference at the locks and in the center of the tape reaches 250 °C after 5 °C. With an increase in the electrical resistance of the shell metal, the heating intensity increases.

According to our experimental data on the thermal state of the powder tape protrusion (Fig. 6), the heating of the protrusion 60 mm long by Joule heat occurs up to 600 °C (in the case of a copper shell – up to 400 °C), after which the arc radiation begins to exert its influence. At the point of contact of the shell with the arc column (at a distance of 2–3 mm from the arc), the protrusion temperature rises abruptly to the melting temperature. The obtained data are optimal and may vary depending on the composition of the filler, the thickness of the shell, the size of the tape, the degree of compression of the shell and the core.

In the literature [5–12], in contrast to our studies, the influence of the bonding layer on the temperature distribution is not taken into account. However, taking into account the presence of the bonding layer is important when predicting the quality of the weld metal when surfacing composite and complex-alloyed alloys. Thus, when surfacing composite alloys, the heating of refractory components of the charge is minimized and their transfer to the welding bath without melting in the initial state is ensured. When surfacing complex-alloyed alloys, the uniformity of heating and melting of the powder electrode is ensured and, accordingly, high chemical homogeneity of the weld metal.

Thus, the assessment of thermal effects taking into account the bonding layer makes it possible to predict the general patterns of the aggregate state, heat and mass transfer,

and phase transitions. That makes it possible to calculate the direction and limits of physicochemical reactions and outline ways to control the power parameters of the powder tape manufacturing process and the characteristics of surfacing mode.

Analytical description of heating patterns makes it possible to solve technological problems under industrial conditions for improving the quality of the deposited metal, increasing the productivity of the process, as well as resource and energy saving when surfacing composite and alloyed wear-resistant alloys. It makes it possible to determine ways to control the thermal state of the powder electrode according to the following options: regulating the heating rate of the shell; changing the heat transfer of the shell to the core due to the connecting layer.

The area of further research into the development of the model is to take into account the preheating of the powder tape from a separate source in the region located above or below the power supply. To implement the model, it is planned to develop a software package that could provide quick and effective visualization of the results of temperature calculation at any point on the powder tape protrusion.

7. Conclusions

1. A mathematical model has been built that makes it possible to determine the dependence of the heating temperature of shell protrusion on the welding current density, dimensions, fill factor, and thermophysical properties of the powder tape, which takes into account the technological features of the electrode manufacturing.

2. According to our results of mathematical modeling, it was determined that the heating temperature of the powder tape protrusion with a length of 40–80 mm during its melting is 400–600 °C for a steel shell, 300–400 °C for a copper shell, which is confirmed by experimental data and indicates the adequacy of the proposed calculation scheme in the mathematical model of the thermal state of the protrusion and its reasonable accuracy for practical calculations.

Conflicts of interest

The authors declare that they have no conflicts of interest in relation to the current study, including financial, personal, authorship, or any other, that could affect the study, as well as the results reported in this paper.

Funding

The study was conducted without financial support.

Data availability

Data sharing not applicable to this paper as no datasets were generated or analyzed during the current study.

Use of artificial intelligence

The authors confirm that they did not use artificial intelligence technologies when creating the current work.

References

1. Yang, X. (2015). Analysis of Chinese Welding Industries Today and in the Future (Focus on Cost, Productivity, and Quality). International Journal of Mechanical Engineering and Applications, 3 (6), 127. https://doi.org/10.11648/j.ijmea.20150306.15
2. Voronchuk, O. P., Zhudra, O. P., Kaida, T. V., Petrov, O. V., Kapitanchuk, L. M., Bogaichuk, I. L. (2022). Influence of the composition of charge components of flux-cored strips of C-Fe-Cr-Nb alloying system on chemical composition and structure of the deposited metal. Automatic Welding, 8, 29–34. https://doi.org/10.37434/as2022.08.04
3. Prysyazhnyuk, P., Ivanov, O., Matvienkiv, O., Marynenko, S., Korol, O., Koval, I. (2022). Impact and abrasion wear resistance of the hardfacings based on high-manganese steel reinforced with multicomponent carbides of Ti-Nb-Mo-V-C system. Procedia Structural Integrity, 36, 130–136. https://doi.org/10.1016/j.prostr.2022.01.014
4. Gribkov, E. P., Perig, A. V. (2016). Research of energy-power parameters during powder wire flattening. The International Journal of Advanced Manufacturing Technology, 85 (9-12), 2887–2900. https://doi.org/10.1007/s00170-016-8714-1
5. Gribkov, E. P., Malyhin, S. O., Hurkovskaya, S. S., Berezshnaya, E. V., Merezhko, D. V. (2022). Mathematical modelling, study and computer-aided design of flux-cored wire rolling in round gauges. The International Journal of Advanced Manufacturing Technology, 119 (7-8), 4249–4263. https://doi.org/10.1007/s00170-022-08662-x
6. Gomes, J. H. F., Costa, S. C., Paiva, A. P., Balestrassi, P. P. (2012). Mathematical Modeling of Weld Bead Geometry, Quality, and Productivity for Stainless Steel Claddings Deposited by FCAW. Journal of Materials Engineering and Performance, 21 (9), 1862–1872. https://doi.org/10.1007/s11665-011-0103-1
7. Mutaşcu, D., Karancsi, O., Mitelea, I., Crăciunescu, C. M., Buzdugan, D., Uțu, I.-D. (2023). Pulsed TIG Cladding of a Highly Carbon-, Chromium-, Molybdenum-, Niobium-, Tungsten- and Vanadium-Alloyed Flux-Cored Wire Electrode on Duplex Stainless Steel X2CrNiMoN 22-5-3. Materials, 16 (13), 4557. https://doi.org/10.3390/ma16134557
8. Guo, N., Zhang, X., Fu, Y., Luo, W., Chen, H., Long He, J. (2023). A novel strategy to prevent hydrogen charging via spontaneously molten-slag-covering droplet transfer mode in underwater wet FCAW. Materials & Design, 226, 111636. https://doi.org/10.1016/j.matdes.2023.111636
9. Trembach, B., Grin, A., Turchanin, M., Makarenko, N., Markov, O., Trembach, I. (2021). Application of Taguchi method and ANOVA analysis for optimization of process parameters and exothermic addition (CuO-Al) introduction in the core filler during self-shielded flux-cored arc welding. The International Journal of Advanced Manufacturing Technology, 114 (3-4), 1099–1118. https://doi.org/10.1007/s00170-021-06869-y

10. Tippayasam, C., Taengwa, C., Palomas, J., Siripongsakul, T., Thaweechai, T., Kaewvilai, A. (2023). Effects of flux-cored arc welding technology on microstructure and wear resistance of Fe-Cr-C hardfacing alloy. Materials Today Communications, 35, 105569. https://doi.org/10.1016/j.mtcomm.2023.105569
11. Świerczyńska, A., Varbai, B., Pandey, C., Fydrych, D. (2023). Exploring the trends in flux-cored arc welding: scientometric analysis approach. The International Journal of Advanced Manufacturing Technology, 130 (1-2), 87–110. https://doi.org/10.1007/s00170-023-12682-6
12. Kannan, T., Murugan, N. (2006). Effect of flux cored arc welding process parameters on duplex stainless steel clad quality. Journal of Materials Processing Technology, 176 (1-3), 230–239. https://doi.org/10.1016/j.jmatprotec.2006.03.157
13. Chen, S. B., Lv, N. (2014). Research evolution on intelligentized technologies for arc welding process. Journal of Manufacturing Processes, 16 (1), 109–122. https://doi.org/10.1016/j.jmapro.2013.07.002
14. Hirata, Y. (1995). Physics of welding (III) - Melting rate and temperature distribution of electrode wire. Welding International, 9 (5), 348–351. https://doi.org/10.1080/09507119509548811
15. Karwa, R. (2020). Heat and Mass Transfer. Springer Singapore. https://doi.org/10.1007/978-981-15-3988-6
16. Forsberg, C. H. (2020). Heat transfer principles and applications. Academic Press. https://doi.org/10.1016/c2014-0-02744-x